0026-895X/05/6701-163–173$20.00
MOLECULAR PHARMACOLOGY
Vol. 67, No. 1
4168/1187047
Mol Pharmacol 67:163–173, 2005
Printed in U.S.A.

Dynamics of Ca^{2+}-Dependent Cl^- Channel Modulation by Niflumic Acid in Rabbit Coronary Arterial Myocytes

Jonathan Ledoux, Iain A. Greenwood, and Normand Leblanc

Department of Physiology, University of Montréal (J.L.), and Research Centre, Montréal Heart Institute (J.L.), Montréal, Québec, Canada; Department of Basic Medical Sciences, Pharmacology & Clinical Pharmacology, St. George's Hospital Medical School, London, United Kingdom (I.A.G.); and Department of Pharmacology, Centre of Biomedical Research Excellence, University of Nevada School of Medicine Reno, Nevada (N.L.)

Received June 23, 2004; accepted September 27, 2004

ABSTRACT

Calcium-activated chloride channels (Cl_{Ca}) are crucial regulators of vascular tone by promoting a depolarizing influence on the resting membrane potential of vascular smooth muscle cells. Niflumic acid (NFA), a potent blocker of Cl_{Ca} in vascular myocytes, was shown recently to cause inhibition and paradoxical stimulation of sustained calcium-activated chloride currents [$I_{Cl(Ca)}$] in rabbit pulmonary artery myocytes. The aims of the present study were to investigate whether NFA produced a similar dual effect in coronary artery smooth muscle cells and to determine the concentration-dependence and dynamics of such a phenomenon. Sustained $I_{Cl(Ca)}$ evoked by intracellular Ca^{2+} clamped at 500 nM were dose-dependently inhibited by NFA (IC_{50} = 159 μM) and transiently augmented in a concentration-independent manner (10 μM to 1 mM) ~2-fold after NFA removal. However, the time to peak and duration of NFA-enhanced $I_{Cl(Ca)}$ increased in a concentration-dependent fashion. Moreover, the rate of recovery was reduced by membrane depolarization, suggesting the involvement of a voltage-dependent step in the interaction of NFA, leading to stimulation of $I_{Cl(Ca)}$. Computer simulations derived from a kinetic model involving low (K_i = 1.25 mM) and high (K_i < 30 μM) affinity sites could reproduce the properties of the NFA-modulated $I_{Cl(Ca)}$ fairly well.

Calcium-activated chloride currents [$I_{Cl(Ca)}$] are expressed in various cell types, including some types of vascular smooth muscle cells, and are considered a key player in the regulation of cell-membrane potential. These currents are evoked by an elevation of intracellular Ca^{2+} concentration ($[Ca^{2+}]_i$) and have distinctive biophysical properties that include a discriminating selectivity pore that conforms to type I Eisenman sequence, voltage-dependent kinetics of activation and deactivation (Greenwood et al., 2001; Ledoux et al., 2003), a calcium sensitivity within the submicromolar range ($EC_{50} \approx$ 365 nM with full activation ≈ 600 nM $[Ca^{2+}]_i$) (Pacaud et al., 1992; Ledoux et al., 2003), and a small single-channel conductance (1–3 pS) with multiple subconductance states (Klöckner, 1993; van Renterghem and Lazdunski, 1993; Hirakawa et al., 1999; Piper and Large, 2003). However the molecular identity of the channel underlying $I_{Cl(Ca)}$ in smooth muscle is still a matter of debate (Britton et al., 2002). Therefore, investigation of the physiological relevance of $I_{Cl(Ca)}$ relies on the effectiveness of pharmacological tools. A number of chemically disparate compounds block $I_{Cl(Ca)}$ in smooth muscle cells ranging from stilbene derivatives (4,4-diisothiocyanato-stilbene-2,2-disulfonic acid) (Hogg et al., 1994b), anthracene-9-carboxylic acid (A-9-C) (Hogg et al., 1994b), and fenamates (flufenamic acid, niflumic acid) (Hogg et al., 1994a; Greenwood and Large, 1995). Niflumic acid (NFA) is a nonsteroidal anti-inflammatory drug that is recognized as the most potent inhibitor of $I_{Cl(Ca)}$ in smooth muscle cells owing to an IC_{50} within the low micromolar range (Hogg et al., 1994a; Greenwood and Large, 1995). Therefore, NFA has been widely used to assess the physiological role of these currents in the regulation of vascular tone (Criddle et al., 1996, 1997; Yuan, 1997; Lamb and Barna, 1998; Remillard et al., 2000; Dai and Zhang, 2001).

However, NFA is not an ideal probe for investigating the

This work was supported by a Doctoral Studentship Award (to J.L.) from the Canadian Institute of Health Research (CIHR), a Wellcome Trust Research Career Development Fellowship (number 53793) (to I.A.G.), and grants from the CIHR (MOP-10863), the Montréal Heart Institute Fund, the Western Affiliate of the American Heart Association (0355060Y), and the Center of Biomedical Research Excellence (COBRE; NCRR 5 P20 RR15581), University of Nevada School of Medicine, Reno, Nevada (to N.L.).

Article, publication date, and citation information can be found at http://molpharm.aspetjournals.org.

doi:10.1124/mol.104.004168.

ABBREVIATIONS: $I_{Cl(Ca)}$, calcium-activated chloride current; NFA, niflumic acid; A-9-C, anthracene-9-carboxylic acid; Cl_{Ca}, calcium-activated chloride channel; ANOVA, analysis of variance; STIC, spontaneous transient inward current; BAPTA, 1,2-bis(2-aminophenoxy)ethane-*N*,*N*,*N*′,*N*′-tetraacetic acid; HP, holding potential.

role of $I_{Cl(Ca)}$, because this agent, along with other members of the fenamate family, modulates a number of other ion channels. Niflumic acid and other fenamates stimulate large-conductance Ca^{2+}-dependent K^+ channels (Hogg et al., 1994a; Ottolia and Toro, 1994; Greenwood and Large, 1995). Flufenamic acid and tolfenamic acids relaxed guinea pig tracheal contractions through a direct inhibition of voltage-gated Ca^{2+} channels (Li et al., 1998). Niflumic acid stimulated Ca^{2+} release from internal stores in rat pulmonary artery smooth muscle cells (Cruickshank et al., 2003) and was shown, along with 5-nitro-2-(3-phenylpropylamino)-benzoic acid and 4,4-diisothiocyanato-stilbene-2,2-disulfonic acid, to inhibit endothelin-1–induced contractions of rat pulmonary arterial myocytes by a mechanism independent of block of Cl_{Ca} channels (Kato et al., 1999). Moreover, the IC_{50} for NFA block of spontaneously occurring $I_{Cl(Ca)}$ is significantly lower than that required to block $I_{Cl(Ca)}$ evoked by caffeine or an agonist such as norepinephrine (Large and Wang, 1996). This phenomenon is extended further when the channel is stimulated by a sustained level of $[Ca^{2+}]$ provided by the pipette solution in which a number of paradoxical effects are observed. In rabbit pulmonary myocytes, NFA only blocked sustained $I_{Cl(Ca)}$ at positive potentials and augmented the tonic current at the holding potential of −50 mV (Piper et al., 2002). Upon washout of NFA, there was a marked enhancement of current amplitude greater than control values that was associated with a marked increase in the activation kinetics. Similar effects were observed for the chemically related agent dichloro-diphenyl 2-carboxylic acid (Piper et al., 2002), whereas A-9-C, which inhibits $I_{Cl(Ca)}$ in a strongly voltage-dependent manner, produced a marked 3-fold increase in the deactivating tail current at −80 mV (Piper and Greenwood, 2003). These data suggest that in pulmonary artery myocytes, fenamate- and A-9-C–induced inhibition of $I_{Cl(Ca)}$ masks a parallel stimulation that is revealed either by washout of the drug (NFA) or by voltage-dependent dissociation from the channel (A-9-C). It is presently unknown whether the NFA-induced stimulation of $I_{Cl(Ca)}$ in pulmonary artery myocytes (Piper et al., 2002) is unique to the vascular smooth muscle preparation. In addition, Piper et al. (2002) have used a slow superfusion system to monitor the effects of NFA on $I_{Cl(Ca)}$, and thus, the true time course of stimulation of this current after washout of NFA is unclear. Finally, information on the concentration dependence of the enhancing effect of NFA on $I_{Cl(Ca)}$ is lacking, because Piper et al. (2002) have only examined the effect of a single concentration of NFA (100 μM).

The aim of the present study was to determine whether a similar anomalous effect of NFA was observed on sustained $I_{Cl(Ca)}$ in rabbit coronary artery myocytes and to investigate the dynamics and concentration dependence of this stimulation using a computer-assisted fast-flow superfusion system. We report here that the relative increase of $I_{Cl(Ca)}$ is independent of drug concentration, whereas the time to reach the maximal stimulation and the duration of the enhanced state increased in a concentration-dependent manner. The rate of recovery from stimulation was also voltage-dependent, with negative potentials accelerating recuperation from enhanced $I_{Cl(Ca)}$. We propose a model whereby NFA stimulates $I_{Cl(Ca)}$ by binding to high- and low-affinity sites, which are occluded by the interaction of NFA with the inhibitory site. Preliminary results have been presented previously (Ledoux and Leblanc, 2002).

Methods and Materials

Isolation of Coronary Myocytes. Cells were freshly dissociated from coronary arteries isolated from New Zealand white rabbits (2–3 kg) that had been killed by anesthetic overdose in accordance with Canadian and U.S. regulations. All animal-handling protocols received the approval of local ethics committees. Arterial myocytes were isolated from the left descending and circumflex coronary arteries. After dissection and removal of connective tissue, the coronary arteries were cut into small strips and placed in a physiological salt solution containing no added Ca^{2+} and 100 μM EGTA at 22°C for 30 min. The coronary arteries were then incubated in a physiological salt solution containing 10 μM Ca^{2+} (no EGTA) and 1 mg/ml collagenase type 2 (Worthington Biochemicals, Lakewood, NJ) and 0.05 mg/ml protease type I (Sigma-Aldrich, St. Louis, MO) for 20 to 25 min at 35°C. In all cases, cells were released by gentle agitation with a wide-bore Pasteur pipette. Cells were stored at 4°C and were used within 6 h.

Electrophysiology. All experiments were carried out at room temperature (22–25°C), and all currents were recorded in the standard whole-cell variant of the voltage-clamp technique using pClamp software (version 8.2; Axon Instruments Inc., Union City, CA) and Axopatch-1D (Axon Instruments). Analysis was performed using the applicable software as well as Origin (version 5.0; OriginLab Corp, Northampton, MA). Current tracings and graph plots were all exported to CorelDraw (version 12; Corel Corporation, Ottawa, ON, Canada) for processing of the figures. Solutions were delivered by gravity through a manifold perfusion system (Cell Micro Controls, Norfolk, VA) controlled by a homemade electronic switch box (Department of Biomedical Engineering, Montreal Heart Institute, Montreal, QC, Canada) that allowed to quickly modify the external medium surrounding the patched myocytes (complete exchange time of <300 ms from measurements of changes in junction potential of a patch pipette when switching from a NaCl-based solution to a KCl-containing solution). Rapid replacement of external solutions was triggered and monitored using a Pentium II personal computer interfaced with a Digidata 1200B acquisition system (Axon Instruments) and pClamp v8.2 software (Clampex).

Solutions. All experiments were carried out in K^+-free media. The external solution contained 130 mM NaCl, 10 mM $NaHCO_3$, 5.4 mM tetraethylammonium chloride, 0.5 mM $MgCl_2$, 5.5 mM glucose, 10 mM HEPES-NaOH, pH 7.35, 1.8 mM $CaCl_2$, and 0.001 mM nifedipine. The pipette solution contained 100 mM cesium aspartate, 20 mM CsCl, 20 mM tetraethylammonium chloride, 5 mM HEPES-CsOH, pH 7.2, 10 mM EGTA, 5 mM Mg-ATP, and 0.2 mM GTP-diNa. Free $[Ca^{2+}]_i$ was adjusted to 500 nM by adding $CaCl_2$ (7.7 mM) and $MgCl_2$ (0.77 mM), with free $[Mg^{2+}]_i$ set to 1 mM, as determined by the software WinMaxC (version 2.1; http://www.stanford.edu/~cpatton). As reported previously (Ledoux et al., 2003), buffered Ca^{2+} concentration in the pipette solution was independently verified using a Ca^{2+}-sensitive electrode (model 93-20; Thermo Orion, Beverly, MA) and calibrated Ca^{2+} solutions available from a commercial source (CALBUF-2; World Precision Instruments, Inc., Sarasota, FL). NFA and all enzymes were purchased from Sigma-Aldrich. NFA was dissolved in dimethyl sulfoxide (NFA stock solution = 100 mM), and the final dimethyl sulfoxide concentration never exceeded 1%, a solvent concentration that did not alter the current in our conditions.

Computer Simulations. The interaction of NFA with Cl_{Ca} channels was mathematically simulated using Markov chain kinetic models, which were resolved numerically by Axon Engineer software (version 2.11c; Aeon Software Inc., Madison, WI) run on Micron TransPort GX$^+$ laptop computer (Pentium III, 700 MHz). Simulations lasting up to 30 s were initiated from a holding potential of −50 mV under non–steady-state conditions. Ordinary differential equations were solved simultaneously by the Gear numerical integration

method using incremental time steps of 10 μs. The specific parameters and equations used in the simulations are listed in Table 1.

Statistical Analysis. All data are the mean ± S.E.M. of n cells from more than two animals. Statistica for Windows 99 (version 5.5; Tulsa, OK) was used to determine statistical significance between groups with one-way ANOVA test followed by a Fisher least significant difference post hoc multiple range tests for repeated measures in multiple group comparisons. $p < 0.05$ was considered to be statistically significant.

Results

Under K^+-free internal and external conditions, coronary myocytes dialyzed with an internal solution containing 500 nM free [Ca^{2+}] generated a sustained current at the holding potential of −50 mV that exhibited distinctive time-dependent outward relaxations upon depolarization followed by an exponentially declining inward current upon repolarization to −80 mV. This current is $I_{Cl(Ca)}$-evoked persistently by the pipette [Ca^{2+}] (500 nM) and has been characterized extensively in previous studies (Greenwood et al., 2001; Ledoux et al., 2003). Figure 1A shows that the application of 100 μM NFA with a fast-flow superfusion system quickly blocked both time-dependent outward current and tail components of $I_{Cl(Ca)}$ (Fig.1A, inset). Inhibition of $I_{Cl(Ca)}$ was observed with all concentrations of niflumic acid with an IC_{50} of 159 ± 48 μM (Fig. 1B). Upon washout of NFA, the current amplitude increased transiently beyond control values, with a mean increase of 50 ± 8, 73 ± 15, and 44 ± 9% for the instantaneous, late, and tail currents, respectively (n = 11). This transient augmentation of current amplitude after a brief pulse of NFA was highly reproducible and could be repeated for the duration of the experiment (Fig. 1A). NFA washout not only modified $I_{Cl(Ca)}$ amplitude but also altered channel opening and closing rates (Fig. 1C, a). Indeed, washout of NFA accelerated the activation kinetics at +90 mV and altered the kinetics of deactivation at −80 mV (Fig. 1C, b and c). In control conditions, the inward current relaxed after a monotonic time course with a time constant (τ) of 38 ± 2 ms but decayed biexponentially after washout of NFA (Fig. 1C, b and c; mean τ values were 193 ± 25 and 21 ± 2 ms, respectively; n = 10). These data show that the anomalous effects of NFA on sustained $I_{Cl(Ca)}$ described previously in pulmonary artery myocytes (Piper et al., 2002) are also apparent in coronary artery cells.

TABLE 1
Parameters used to compute the mathematical model describing the inhibition and stimulation of $I_{Cl(Ca)}$ by niflumic acid

	Units
Permeability and selectivity	
$P_{Cl(Ca)}$ max = 0.01	$\mu M\ ms^{-1}$
$E_{Cl} = -30$	mV
Values of gating variables	
C = 0.6	
O_1 = 0.7	
B_1 = 0	
B_2 = 0	
O_2 = 1	
O_3 = 1	
Activation and deactivation	
α_1 (V) = 0.0075/{1 + exp [−0.1 * (V − 50)]}	ms^{-1}
β_1 (V) = 0.1 /{1 + exp [0.1 * (V + 80)]}	ms^{-1}
High-affinity binding of NFA and unbinding	
α_2 ([NFA]) = $[NFA]^2/([NFA]^2 + 0.023^2)$	ms^{-1}
β_2 = 0.5	ms^{-1}
α_3 = 0.058	ms^{-1}
β_3 ([NFA]) = 0.05*{[NFA]/{[NFA] + 0.01}	ms^{-1}
Low-affinity binding of NFA and unbinding	
α_4 ([NFA])= 0.00325*{[NFA]/{[NFA] + 1.25}	ms^{-1}
α_5 = 0.0004	ms^{-1}
Recovery from high affinity and fast binding of NFA	
α_6 = 0.0006	ms^{-1}
Recovery from low affinity and slow binding of NFA	
α_7 = 0.0001	ms^{-1}

E_{Cl}, equilibrium potential for chloride ions.

Concentration-Dependence of NFA-Induced $I_{Cl(Ca)}$ Stimulation. The concentration- and time-dependence of the NFA stimulatory effect were performed on cells maintained at a test potential of +60 mV for 20 s and exposed to different concentrations of NFA (1 μM, 10 μM, 100 μM, and 1 mM) for durations between 2 and 10 s. Enhancement of $I_{Cl(Ca)}$ was only observed after washout of higher NFA concentrations greater than 1 μM (Fig. 2, B–D). Moreover, the kinetics of the enhanced current was strongly dependent on the applied NFA concentration. Thus, the enhanced $I_{Cl(Ca)}$ generated upon washout of 10 μM NFA decayed monophasically after reaching its peak (Fig. 2B), whereas the relaxation of the stimulated current after removal of 100 μM NFA displayed a sustained phase superimposed on an initial rapid component (Fig. 2C). After washout of 1 mM NFA, the onset of stimulation was characterized by a markedly reduced rapid component followed by a slowly developing sustained phase of stimulation (Fig. 2D).

The relative increase of $I_{Cl(Ca)}$ amplitude upon washout of NFA did not vary as a function of the concentration of NFA applied. Thus, after 2-s applications in the same cell of 10 μM, 100 μM, and 1 mM NFA, $I_{Cl(Ca)}$ increased 1.9 ± 0.3-, 2.1 ± 0.3-, and 2.0 ± 0.2-fold, respectively. In contrast, the delay between the washout of drug and the maximal enhanced $I_{Cl(Ca)}$ increased in a concentration-dependent manner (highlighted in the inset of Fig. 3B). The time to reach the peak current increased significantly from 0.27 ± 0.03 s after washout of 10 μM NFA to 0.6 ± 0.2 and 7 ± 1 s after washout of 100 μM and 1 mM NFA, respectively (n = 7). Moreover the duration of the transient stimulated current upon washout of NFA was also concentration-dependent (Figs. 2 and 3C). The time for the stimulated current to decay by 50% of the maximal amplitude increased from 0.45 ± 0.03 s after washout of 10 μM NFA to 0.74 ± 0.08 and 14 ± 1 s after removal of 100 μM and 1 mM NFA, respectively. From Figs. 2 and 3, it is obvious that for each NFA concentration, the washout enhancement was not affected by changes in the duration of NFA application. These results highlight the complex dynamics associated with the stimulation of $I_{Cl(Ca)}$ produced by the washout of NFA.

Voltage-Dependence of NFA-Enhanced $I_{Cl(Ca)}$. We next sought to determine the voltage-dependence of the stimulation of $I_{Cl(Ca)}$ by NFA. In this series of experiments, cells were exposed to 100 μM NFA while being held at different membrane potentials (i.e., −60, +20, +60, and + 90 mV) from a holding potential of −50 mV (Figs. 4, A–C, and 5). These experiments revealed that the peak increase in $I_{Cl(Ca)}$ induced by a 10-s exposure to NFA was similar at all voltages examined (Fig. 5A). Shorter applications (2–8 s) of NFA revealed a similar pattern (data not shown). There was a trend, although not significant, that the time to peak stimulated current upon washout of NFA increased with membrane depolarization (Fig. 5B). However, the time course of the stimulated current was clearly prolonged at positive relative

to negative potentials, as evident from an analysis of the area under the curve of the stimulated current (Fig. 5C). Moreover, at +90 mV, there was no significant decay of the stimulated current for the duration of this experiment (Fig. 4A).

Identity of NFA-Enhanced Current. It could be postulated that the current elicited upon washout of NFA was caused by the de novo recruitment of a previously silent channel as opposed to modulation of an existing one. Therefore, experiments were undertaken to determine whether the stimulated current was as equally sensitive to NFA as the control $I_{Cl(Ca)}$. Figure 6A shows a representative experiment in which a cell was stepped to +60 mV, and then NFA was applied for 2 s. It can be seen clearly that the stimulated current evoked upon washout is rapidly inhibited by a repeat application of NFA to an extent observed for the control current. Similar results were observed in three other cells. Further experiments were undertaken to determine the reversal potential of the current evoked upon washout of NFA. Approximately 500 ms after the application of NFA for 2 s, a ramp change in voltage (−50 to +50 mV, 250 ms) was imposed. The reversal potentials of the enhanced $I_{Cl(Ca)}$ recorded from cells bathed previously in 100 μM (−15.8 ± 1.7 mV, n = 6) or 1 mM NFA (−18.5 ± 1.6 mV, n = 4) do not significantly differ from each other and are close to the theoretical value for the Cl^- equilibrium potential under our conditions (Greenwood et al., 2001; Ledoux et al., 2003). These data support the hypothesis that NFA is modulating an existing Cl^- channel.

Mathematical Modeling of NFA Interactions with $I_{Cl(Ca)}$. The experimental effects of NFA were simulated mathematically using a computer-modeling method similar to that reported previously by our group (Remillard and Leblanc, 1996). Figure 7 displays the various kinetic schemes that were tested. Because the myocytes were dialyzed with a fixed intracellular Ca^{2+} concentration set at 500 nM, we simplified our theoretical analysis by focusing on the possible steps by which NFA interacts with the channels, although we recognize that a more elaborate model of the channel (Arreola et al., 1996; Kuruma and Hartzell, 2000) will have to be evaluated in the future. For all schemes tested, opening of the Ca^{2+}-activated Cl^- channel was modeled by single voltage-dependent reversible transition from closed (C) to open (O_1). Although a simple binding site model assuming a single binding site leading to block and stimulation (Fig. 7A) could fairly well reproduce the block and transient stimulation of $I_{Cl(Ca)}$ at 10 μM NFA, it could not account for the biphasic stimulation of $I_{Cl(Ca)}$ with 100 μM and 1 mM NFA. Alternative schemes were tested that assumed the existence of one inhibitory state and one (Fig. 7, B and C) or two (Fig. 7, D–F) stimulatory binding sites. For all of the schemes shown in Fig. 7, B through F, application of NFA first interacts with a binding site leading to current inhibition (B_1). State B_1 occludes the stimulation unless the drug is washed out quickly. We tested several scheme variants, which included a common high-affinity blocking and stimulatory state and a low-affinity stimulatory state (Fig. 7C), different schemes with a

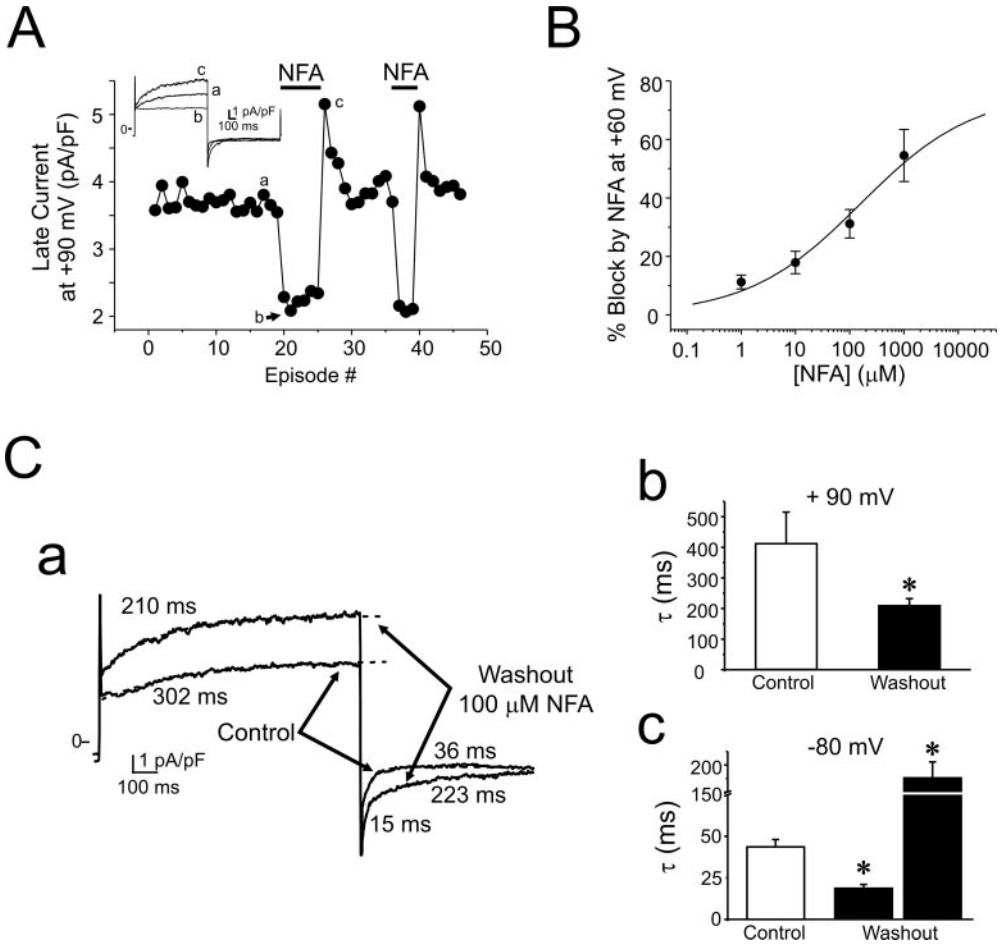

Fig. 1. Block and stimulation of Ca^{2+}-activated Cl^- current by niflumic acid in rabbit coronary myocytes dialyzed with 500 nM $[Ca^{2+}]_i$. A, time course of peak outward current recorded at +90 mV every 10 s in coronary smooth muscle cells dialyzed with 500 nM $[Ca^{2+}]_i$; 100 μM NFA (NFA) was applied using a fast-flow superfusion system for the period denoted by the bar. Inset, sample traces obtained in control (a), presence (b), and after washout of 100 μM NFA (c), respectively. B, concentration-dependence of the inhibitory effects of NFA on $I_{Cl(Ca)}$ recorded at +60 mV. Data were obtained from experiments similar to those illustrated in Fig. 2. The solid line passing through the points is a logistic function fit to the data with the following parameters: $Y = 76.1/[1 + (x/159)^{0.42}]$. NFA concentrations are equal to 1 μM, 10 μM, 100 μM, and 1 mM, n = 11, 7, 7, and 7, respectively. C, effects of NFA removal on activation and deactivation kinetics of $I_{Cl(Ca)}$. a, sample traces of $I_{Cl(Ca)}$ evoked by the protocol used in A in the absence (control) and after washout of 100 μM NFA. b and c, bar graphs representing the mean time constants of activation (+90 mV) and deactivation (−80 mV), respectively, before (control) and after (washout) exposure to 100 μM NFA of experiments similar to those shown in a (n = 10).

single inhibitory site, and two stimulatory binding sites with different affinities for NFA (Fig. 7, D–F). Although these kinetic schemes were able to account for some aspects of the stimulation mediated by NFA, none of these could fairly well reproduce the concentration- and time-dependence of the block and enhancement of the current by this substance.

Figure 7G shows the model that best reproduced our experimental data. The equations describing the rate constants and other parameters used in the simulations are listed in Table 1. α_n and β_n are the rate constants for the kinetic transitions shown. The gating variables of the stimulated states O_2 and O_3, which are modeled as equivalent states, were set to 1. The fully activated nonstimulated open state O_1 was arbitrarily fixed at 0.7, although efforts to modify even slightly the gating values of the stimulated and nonstimulated states led to failure to model the interaction of NFA with the anion channel. Activation and deactivation were modeled by voltage-dependent transitions described by Boltzmann relationships. The model assumes the existence of high- (ranging from 10 to 23 μM) and low- (1.25 mM) affinity binding sites as indicated in Fig. 7G. Binding of NFA was modeled using the Hill equation with a Hill coefficient of 1 ($O_1 \rightarrow B_2$, $O_2 \rightarrow B_1$) or 2 ($O_1 \rightarrow B_1$). The rate of unbinding of NFA from all bound states and the rates of recovery from stimulated to nonstimulated states were all assumed to be independent of NFA concentration.

Figure 8, A and B, show simulated current traces derived from the model with the four concentrations of NFA tested in our experiments elicited in response to 2- (Fig. 8A) or 6-s (Fig. 8B) exposure to the drug, as indicated below the normalized current traces. The voltage-clamp protocol shown at the bottom was identical with that used in the experiments described in Fig. 2. The simulations were all initiated under non–steady-state conditions, which is why the gating variable for the closed state was set to 0.6. This allowed the simulation to begin with already active channels at the holding potential (−50 mV) in myocytes dialyzed with 500 nM Ca^{2+} or greater, as shown previously by our group (Greenwood et al., 2001; Ledoux et al., 2003). Consistent with this scheme, step depolarization to +60 mV evoked an instanta-

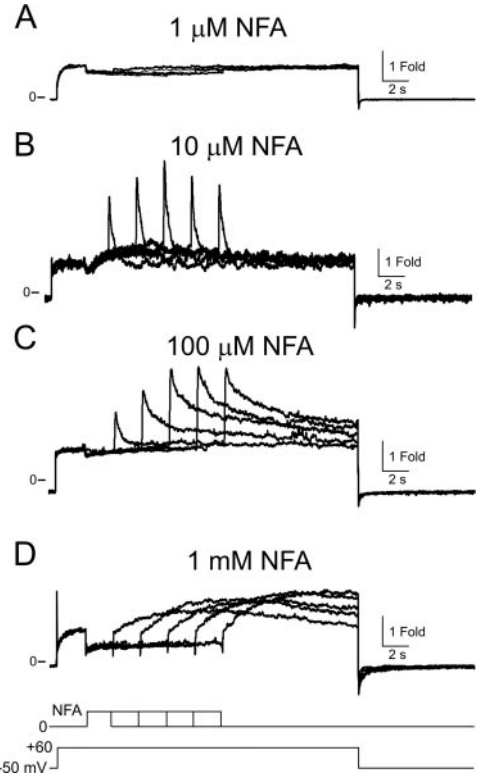

Fig. 2. Dynamics of the stimulated current evoked upon washout of NFA. Sample traces of $I_{Cl(Ca)}$ evoked by a 22-s depolarizing step to +60 mV (HP = −50 mV) followed by a repolarizing step to −50 mV for 8 s every 60 s (A–C) or 90 s (D), as displayed at the bottom of the figure. After 2 s, 1 μM, 10 μM, 100 μM, or 1 mM NFA (A, B, C, and D, respectively) was applied for increasing durations (2-s increments) using a fast-flow superfusion system. Vertical calibrations express the ratio of current amplitude relative to the level reached immediately before the application of NFA.

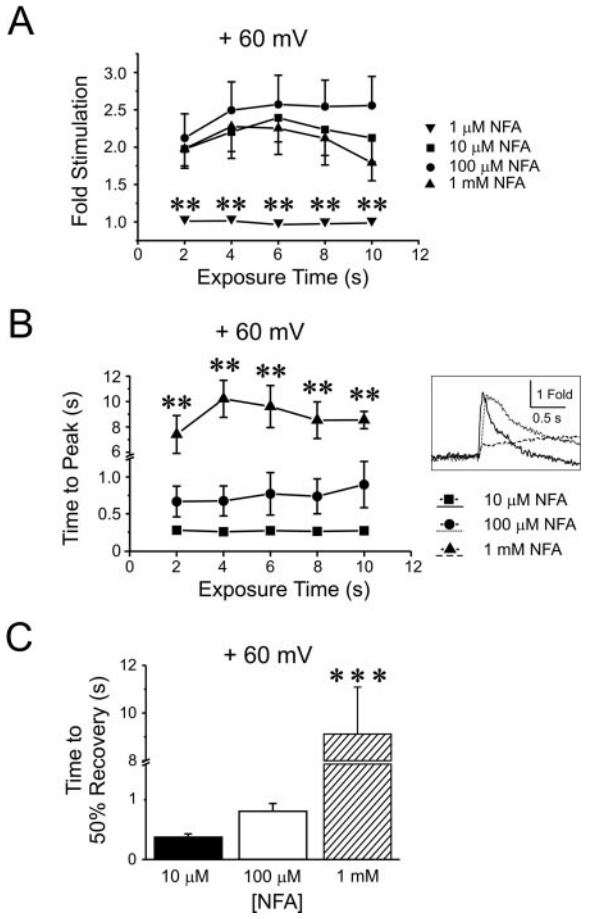

Fig. 3. Concentration dependence of enhanced $I_{Cl(Ca)}$ dynamics induced by NFA washout in coronary myocytes depolarized to +60 mV. A, plot reporting the mean relative increase of $I_{Cl(Ca)}$ in coronary myocytes induced by washout of NFA (1 μM, 10 μM, 100 μM, and 1 mM, n = 11, 7, 7, and 7, respectively) calculated as the peak current amplitude at +60 mV after removal of NFA normalized to the current value before the application of NFA (for 2–10 s), as described in Fig. 2. ANOVA statistical analysis for repeated measures revealed a significant difference between the groups; ⋆⋆, $p < 0.01$. B, graph illustrating the time delay between the washout of drug and the peak amplitude of enhanced $I_{Cl(Ca)}$ after washout of NFA (10 μM, 100 μM, and 1 mM, n = 7) applied for 2 to 10 s. Inset, magnified view of sample traces of cells exposed to 10 μM, 100 μM, and 1 mM NFA for 2 s to illustrate the concentration-dependent time to peak amplitude of enhanced $I_{Cl(Ca)}$. ANOVA statistical analysis for repeated measures revealed a significant difference between the groups; ⋆⋆, $p < 0.001$. C, bar graph showing the mean decay kinetics of enhanced $I_{Cl(Ca)}$ in cells exposed to 10 μM, 100 μM, and 1 mM NFA for 2 s. The time-dependent relaxation was calculated as the period required for peak enhanced $I_{Cl(Ca)}$ to decrease by 50%. One-way ANOVA statistical analysis revealed a significant difference between the three groups; ⋆⋆⋆, $p < 0.001$.

neous current followed by a time-dependent $I_{Cl(Ca)}$ component (Greenwood et al., 2001; Ledoux et al., 2003) (this study, Figs. 1, 2, 4, and 6) that was well-fitted by a single exponential with a time constant of 220 ms, a value similar to that published previously (Greenwood et al., 2001; Ledoux et al., 2003). Application of NFA caused a rapid concentration-dependent block of the current that was more potent than actual data. Maximum block estimated by curve fitting to a logistic function for experimental data, and the model was 62 ± 5 and 96 ± 5%, respectively. The model yielded a K_i value that is approximately 5-fold lower (31 μM) than that calculated from actual data (159 μM). All attempts to adjust the parameters of the model listed in Table 1 to match the blocking ability of NFA to our measurements had deleterious consequences on the time- and dose-dependence of the NFA-induced stimulation of the current, which was the main focus of our analysis.

Whereas washout of 1 μM NFA elicits little effect on the modeled current, washout of this drug when applied at concentrations in the range of 10 μM to 1 mM leads to a transient stimulation that reproduces our data reasonably well. Stimulated currents after washout of 10 or 100 μM NFA were much more transient than those evoked after exposure to 1 mM. It is noteworthy that a longer exposure to 100 μM NFA clearly led to a biphasic relaxation of the current (Fig. 8B, third trace from the top) as observed in experiments (Fig. 2C). The biphasic nature of the stimulated current after washout of 1 mM NFA, characterized by a rapid phase followed by a very slow component (Fig. 2D), is also well accounted for by the model (Fig. 8B, fourth trace from top). Partial recovery of the current after the rapid onset of block was often observed during the application of NFA in the range of 10 μM to 1 mM (Fig. 2, B–D). The model qualitatively reproduces this behavior with 100 μM and 1 mM NFA (Fig. 2B, second and third traces), which suggests that channels blocked by NFA (B_1 and B_2) may partially transit to the stimulated states (O_2 and O_3). Finally, the model is also able to simulate the impact of a double NFA exposure on the current (compare Figs. 8C and 6A), which again supports the

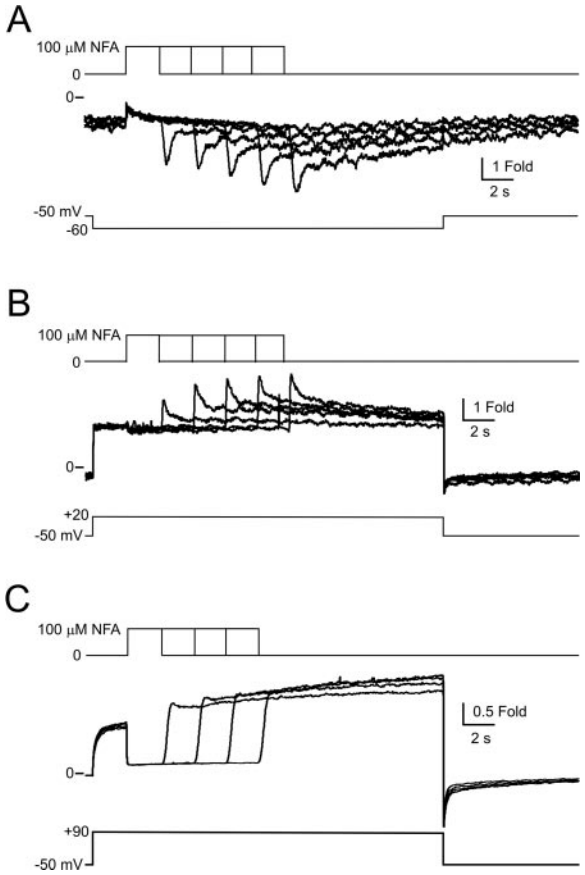

Fig. 4. Voltage dependence of the enhanced $I_{Cl(Ca)}$ after washout of NFA. A, sample traces of $I_{Cl(Ca)}$ evoked by a 22-s step to −60 mV (HP = −50 mV) followed by a repolarizing step to −50 mV for 8 s every 60 s, as displayed under the traces. After 2 s, cells were exposed to 100 μM NFA for 2 s up to 10 s, with 2-s increments followed by the rapid removal of drug from the external medium using a fast-flow superfusion system as depicted over the traces. B and C, similar to A, except that the cells were depolarized to +20 and +90 mV for 22 s (B and C, respectively), as illustrated under the traces.

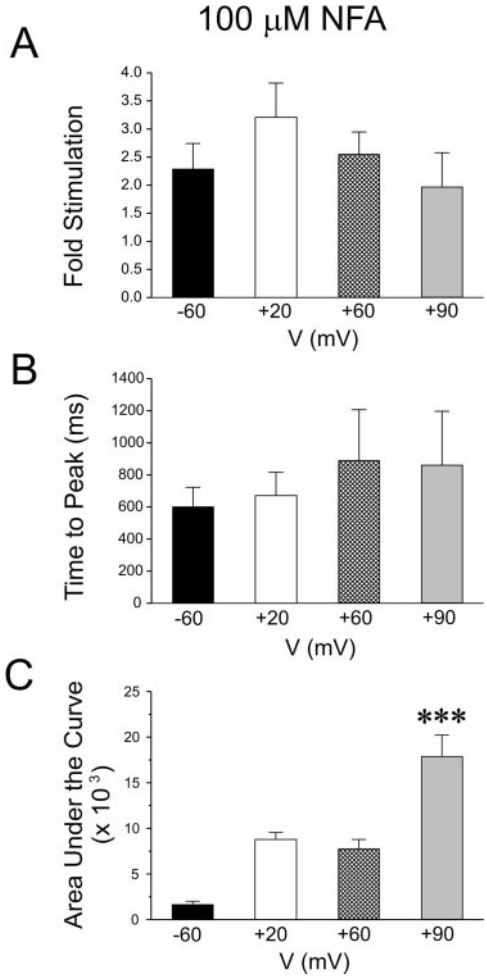

Fig. 5. Quantitative analysis of the voltage-dependence of enhanced $I_{Cl(Ca)}$ induced by 100 μM NFA washout in coronary myocytes. A, Bar graph reporting the mean relative increase in $I_{Cl(Ca)}$ induced after washout of 100 μM NFA applied for 10 s in myocytes held at −60 (■), +20 (□), +60 (▨), and + 90 mV (▤) (n = 5, 5, 7, and 5, respectively) and calculated as the peak current amplitude after removal of NFA normalized to the current value just before exposure to drug, as described in Fig. 4. B, bar graph summarizing the mean delay in milliseconds between the removal of drug and the peak amplitude of enhanced $I_{Cl(Ca)}$ after washout of 100 μM NFA applied for 10 s in myocytes held at −60 (■), +20 (□), +60 (▨), and +90 mV (▤) (n = 5, 5, 7, and 5, respectively). C, bar graph reporting the mean integrated current stimulated by NFA washout measured at −60 (■), +20 (□), +60 (▨), and +90 mV (▤) (n = 5, 5, 7, and 5, respectively). One-way ANOVA statistical analyses revealed a significant difference between the three groups; ⋆⋆⋆, $p < 0.001$.

concept that the control and stimulated currents are produced by the same underlying channels exhibiting distinct behaviors.

Figure 9 illustrates a quantitative comparison of the effects of NFA on recorded and simulated $I_{Cl(Ca)}$. Experimental and model data points are shown as filled and empty symbols. Except for a progressive increase of the simulated current as a function of exposure time to NFA with 1 mM (Fig. 9A, b) that diverged from the measured current, which decreased after NFA exposure times longer than 6 s, the model adequately describes the steep concentration dependence of the stimulation between 1 μM and 1 mM; simulated data points generally fell within one standard deviation for each average measurement. Modeling this abrupt relationship could only be achieved by increasing the Hill coefficient to 2 in the equation describing the rate constant α_2 (Fig. 7G and Table 1) of the high-affinity binding site, which suggests that two or more NFA molecules may be necessary to induce stimulation. Figure 9B shows plots illustrating the time-dependent behavior of simulated versus measured $I_{Cl(Ca)}$. Measurements were carried out at washout times that elicited peak stimulated currents for each of the three NFA concentrations, which were applied for 2 s. These graphs show reasonable agreement between the data and model with all three NFA concentrations, except for a discrepancy observed at the earliest washout time with 100 μM.

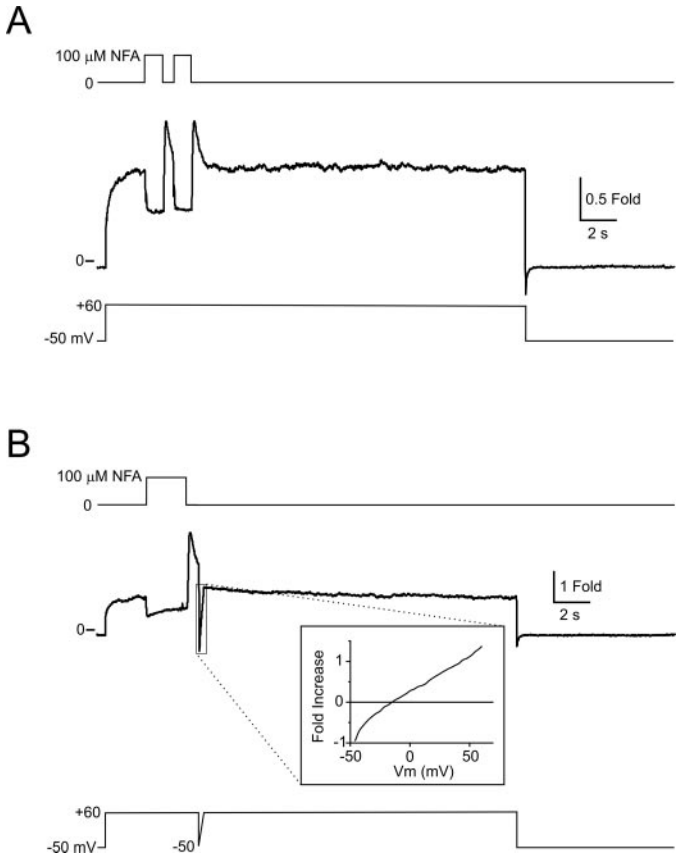

Fig. 6. Properties of NFA-enhanced $I_{Cl(Ca)}$. A, effect of a 2-s application of NFA on $I_{Cl(Ca)}$ recorded at +60 mV. Approximately 500 ms after washout of NFA, the augmented current was blocked by a subsequent application of NFA to a similar degree as the control current. B, generation of a ramp change in voltage 4.5 s after washout of NFA allowed the reversal potential of the stimulated current to be determined. Inset, relative current amplitude plotted as a function of the membrane potential imposed by the ramp protocol (reversal potential in this cell was −16 mV).

Discussion

Niflumic Acid Exerts a Dual Influence on Cl_{Ca} Channels in Coronary Myocytes. A number of chemically diverse agents block Ca^{2+}-activated Cl^- channels, and NFA is unequivocally considered to be the most potent blocker of this conductance in vascular smooth muscle cells (Large and Wang, 1996). The data reported herein show that in coronary artery myocytes, a sustained Ca^{2+}-activated Cl^- current characterized extensively in previous reports is modulated in a paradoxical manner by the chloride-channel blocker niflumic acid. Analysis of the dose-dependent block of $I_{Cl(Ca)}$ revealed an IC_{50} value that was higher (159 μM) than that determined for the inhibitory action of NFA upon spontaneous transient inward currents (STICs) (~2–5 μM) (Hogg et al., 1994a; Greenwood and Large, 1995), which results from the transient activation of Cl_{Ca} channels by Ca^{2+} sparks (Gordienko et al., 1999). This diminished potency of NFA to inhibit $I_{Cl(Ca)}$ was also noticed by Piper et al. (2002) in rabbit pulmonary myocytes dialyzed with elevated $[Ca^{2+}]_i$ (250 nM to 1 μM). Whether the higher efficacy of NFA for blocking STICs relative to $I_{Cl(Ca)}$ elicited by a sustained elevated intracellular Ca^{2+} level is caused by the much higher Ca^{2+} concentrations (tens of micromolar) generated by Ca^{2+} sparks (Jaggar et al., 2000) or the ability of NFA to interfere with Ca^{2+} release from internal stores (Cruickshank et al., 2003) remains to be investigated. An alternative possibility is

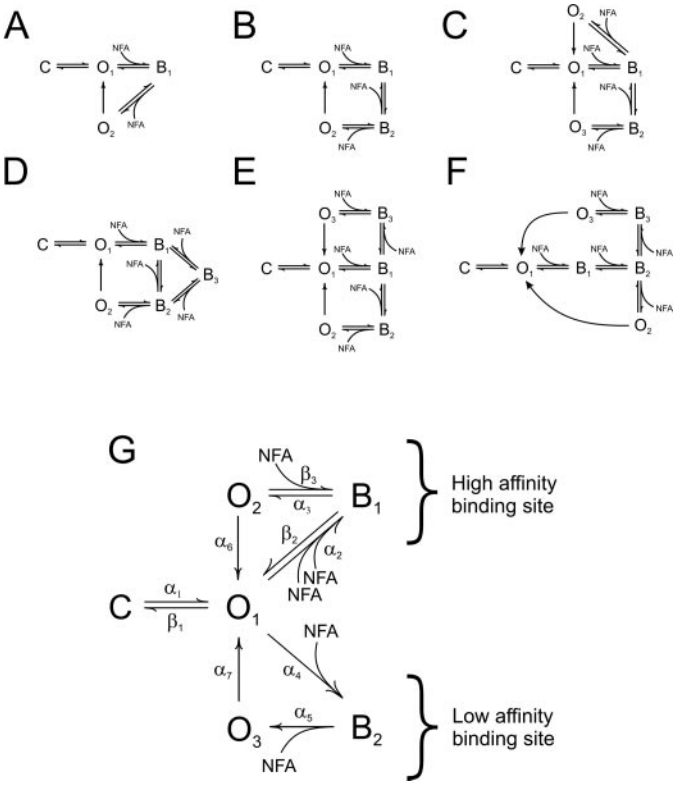

Fig. 7. The different kinetic schemes tested in computer simulations. C, O_n, and B_n reflect closed, open, and blocked kinetic states, respectively. In G, α_n and β_n are the forward and backward rate constants describing the individual state transitions, respectively. The equations describing all the rate constants shown on this scheme are listed in Table 1.

that under conditions of a sustained increase in $[Ca^{2+}]_i$, NFA may stimulate the Cl^- channels, an effect that would be partially obstructed by the inhibition. The study by Piper et al. (2002) demonstrated that washout of NFA enhances $I_{Cl(Ca)}$ in pulmonary myocytes and postulated that the higher open probability of Cl_{Ca} channels elicited by a sustained increase in $[Ca^{2+}]_i$ may tilt the balance toward the stimulatory effect. Our data support this hypothesis, because the rapid block exerted by NFA was often followed by a partial recovery of the current, which suggests that the net current recorded with NFA was the product of a superimposed inhibition and stimulation by the drug.

NFA at concentrations between 10 μM and 1 mM produced an ≈2-fold increase in $I_{Cl(Ca)}$ elicited by 500 nM $[Ca^{2+}]_i$. Although the relative increase of $I_{Cl(Ca)}$ was independent of NFA concentration, the time to reach the peak current increased in a concentration-dependent manner. Furthermore, the time needed to recover from the enhanced state increased in a concentration-dependent manner. These data reflect an anomalous modulation of a Ca^{2+}-activated Cl^- channels by NFA because the NFA-increased current reversed near the predicted equilibrium potential for chloride ions, confirming that the underlying channels were permeable to Cl^-. Moreover, the current enhanced by NFA was equally blocked by a second exposure to this compound. These findings corroborate the earlier observations of Piper et al. (2002) showing

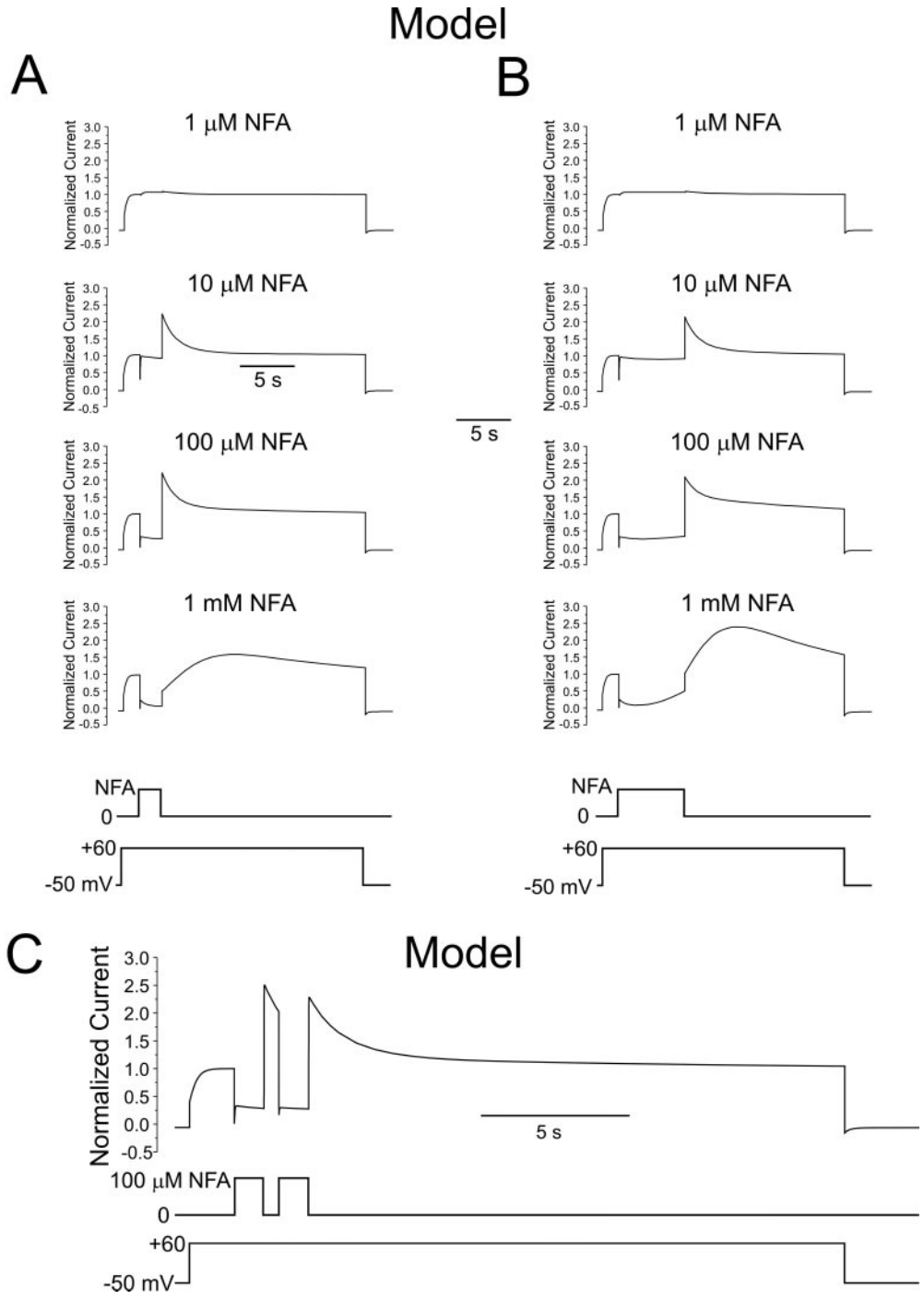

Fig. 8. Simulation of the effects of niflumic acid on Ca^{2+}-activated Cl^- currents using the model described in the text. A, normalized simulated currents elicited by 22-s voltage-clamp steps to +60 from holding potential of −50 mV (bottom trace). In these simulations, a 2-s exposure to either 1 μM (top trace), 10 μM (second trace from the top), 100 μM (third trace from the top), or 1 mM (fourth trace from the top) NFA was implemented 2 s after membrane potential was stepped to +60 mV, as illustrated by the trace immediately above the voltage-clamp protocol. B, identical to A, except that each concentration of NFA was applied for 6 s. C, simulation showing the effect of a double exposure to 100 μM NFA. The two exposures (middle trace) lasted 1 s each and were interspersed by a 500-ms gap. The voltage-clamp protocol shown at the bottom was identical with those described in A and B.

that the current generated by the removal of NFA was not caused by the de novo activation of another conductance.

Voltage-Dependence of NFA-Enhanced Anion Current. The relative magnitude of NFA-enhanced $I_{Cl(Ca)}$ was independent of membrane potential in the range of −60 to +90 mV. However, the rate of current recovery after NFA washout was clearly voltage-dependent, with membrane depolarization delaying the return of the current to baseline. One possibility to explain these results is that the dissociation of NFA is voltage-dependent, with membrane depolarization reducing the rate of unbinding from its binding site(s). An interaction of this drug with the hydrophilic channel pore or extracellular vestibular portion has been postulated (Hogg et al., 1994a; Greenwood and Large, 1995). Piper et al. (2002) showed that intracellular application of NFA (100 μM) was ineffective at modifying $I_{Cl(Ca)}$ in pulmonary myocytes, supporting the idea that NFA modulates Cl_{Ca} channels by accessing one or several binding sites located primarily near the outer mouth of the channel pore. It is possible that NFA may be interacting with a binding site(s) through an electrostatic interaction that is modulated by the transmembrane electric field or by the state of Ca^{2+}- and voltage-dependent gating of the channels.

Mechanism of Action of Niflumic Acid on Cl_{Ca} Channels. Until the molecular nature of native Ca^{2+}-activated Cl^- channels is resolved, we can only speculate on the possible mechanism by which NFA mediates its effects on the channels. It is possible that the stimulation by NFA is caused by a leftward shift of the voltage-dependence of $I_{Cl(Ca)}$, leading to saturation at higher $[Ca^{2+}]_i$, although we cannot rule out the recruitment of silent channels and/or an increase in single-channel conductance. In agreement with this idea, Piper et al. (2002) showed that the stimulatory effects of NFA were abolished by increasing $[Ca^{2+}]_i$ from 500 nM to 1 μM in pulmonary myocytes, which would increase the voltage-dependent availability of $I_{Cl(Ca)}$. On the other hand, NFA could exert a dual effect by inhibiting both Cl_{Ca} channels and the ryanodine and/or inositol 1,4,5-trisphosphate Ca^{2+}-release channels. In the presence of NFA, Cl_{Ca} channels would be blocked, and the slow-release Ca^{2+} load would increase because of reduced Ca^{2+} leakage. Stimulation of $I_{Cl(Ca)}$ after washout of NFA would then result from a transient subsarcolemmal Ca^{2+} release event produced by relief of block of the Ca^{2+}-release channels, even though bulk-free $[Ca^{2+}]_i$ is highly buffered by BAPTA. Arguments against this hypothesis are 1) our inability to ever detect STICs in our experiments; 2) the time course of stimulation of $I_{Cl(Ca)}$ by NFA was highly voltage-dependent (Fig. 5); and 3) NFA was recently shown to enhance rather than inhibit Ca^{2+} release in rat pulmonary myocytes (Cruickshank et al., 2003).

Although the hypothesis of a single binding site is possible, we rather favor the hypothesis that NFA is interacting with more than one binding site, each with different affinities. We carried out mathematical simulations that might account for our observations. Only the working model shown in Fig. 7G could well describe most of the properties of NFA-modulated $I_{Cl(Ca)}$ in our preparation. At low concentrations of NFA ($\leq$ 10 μM), the molecules would only bind to the high-affinity site, which would cause a conformational change in the protein, leading to enhanced activity, but this effect would be mostly masked by channel occlusion. A small but significant number of channels would enter the stimulated state O_2 and thus lead to reduced blockade by the compound. When NFA is washed out, most channels would return to the normal control open state O_1, whereas others that have adopted a new conformational change favoring stimulation would transit to O_2; the slow and transient nature of $I_{Cl(Ca)}$ would arise from the slow unbinding of NFA ($B_1 \rightarrow O_2$) and slow rate constant

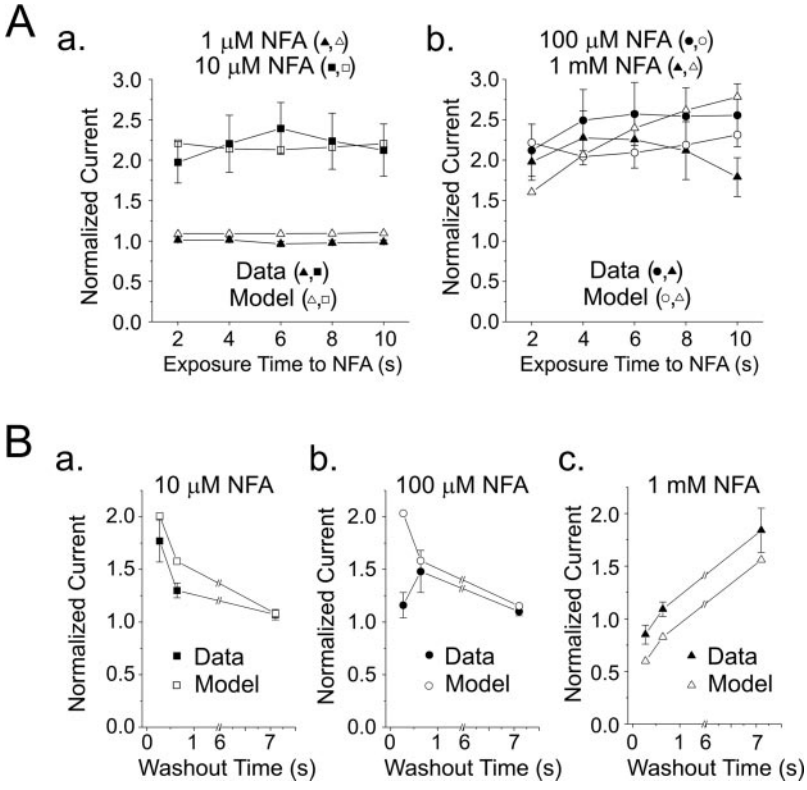

Fig. 9. Comparison of the effects of NFA on recorded and simulated $I_{Cl(Ca)}$. A, graphs showing the time- and dose-dependence of the NFA-induced stimulation of recorded and simulated $I_{Cl(Ca)}$ after washout of the drug. Experimental data points are reproduced from Fig. 3. A 22-s step to +60 mV was applied from HP = −50 mV. Two seconds after the onset of the depolarizing step, NFA was applied for between 2 and 10 s at the concentrations indicated at the top of each graph. The fairly good correlation between experimental (filled symbols) and simulated (open symbols) data is noteworthy. B, graphs showing the time course of NFA-enhanced recorded (filled symbols) and simulated (empty symbols) $I_{Cl(Ca)}$ after washout of 10 μM (a), 100 μM (b), or 1 mM (c) NFA (2-s exposure). The selected washout times chosen correspond to the time to peak measurements taken from the experiments described in Fig. 3. Except for the earliest washout time point with 100 μM NFA, in which a significant deviation was noticed, the model generally reproduced the experimental data well.

describing the return of the stimulated state to the normal state ($O_2 \rightarrow O_1$). At 100 μM NFA, some NFA molecules are beginning to interact with a second lower-affinity binding site that also leads to block (B_2) and stimulation (O_3). The very slow kinetics of unbinding of NFA ($B_2 \rightarrow O_3$) and recovery of the current from the stimulated state ($O_3 \rightarrow O_1$) could explain the appearance of a slower kinetically distinct phase of transient stimulation of $I_{Cl(Ca)}$ after washout of NFA. This becomes even more apparent after washout of 1 mM NFA. The onset of stimulation is now clearly biphasic with a rapid and a slow phase, both of which are well described by the model. The enhanced contribution of a slower phase with a correspondingly reduced rapid component is also consistent with the existence of two mutually exclusive binding sites.

Although useful as an initial working hypothesis to describe the complex interaction of NFA with native Cl_{Ca} channels, the model offers no clues on the molecular mechanisms that are involved in the NFA-induced alterations in channel activity. So far, two kinetic models have been postulated to describe the Ca^{2+}- and voltage-dependence of Ca^{2+}-activated Cl^- channels in parotid acinar cells (Arreola et al., 1996) and *Xenopus laevis* oocytes (Callamaras and Parker, 2000; Kuruma and Hartzell, 2000). These two models are divergent in that one assumes that activation of Cl_{Ca} channels by voltage-dependent binding of several Ca^{2+} ions (Arreola et al., 1996; Callamaras and Parker, 2000) whereas the other postulates that Ca^{2+} binding is voltage-independent, whereas unbinding involves a voltage-dependent step (Kuruma and Hartzell, 2000). Unfortunately, such a detailed description of the behavior of Cl_{Ca} channels in vascular smooth muscle is still pending and is complicated by the very small unitary conductance of the channels (~1–3 pS) (Klöckner, 1993; van Renterghem and Lazdunski, 1993; Large and Wang, 1996; Hirakawa et al., 1999; Piper and Large, 2003) and the fact that they are regulated by phosphotransferase reactions involving calmodulin-dependent protein kinase II (Greenwood et al., 2001) and calcineurin (Ledoux et al., 2003), both of which are activated by intracellular Ca^{2+}. Although additional experiments are required to answer this question, a likely explanation for the effects of NFA may be that the antagonist promotes Ca^{2+} binding and/or reduces the unbinding of Ca^{2+}, one of which is voltage-dependent, leading to an increase in the open probability. Consistent with this hypothesis was the observation that activation and deactivation kinetics of $I_{Cl(Ca)}$ were, respectively, enhanced and reduced after washout of NFA, and this is similar to the effects of an elevation of intracellular Ca^{2+} to near saturation levels on $I_{Cl(Ca)}$ in other cell types (Arreola et al., 1996; Kuruma and Hartzell, 2000).

Pharmacological Relevance of Our Findings. Determination of the role of Cl_{Ca} channels in vascular smooth muscle has been hampered by the lack of truly specific pharmacological probes. Our data provide evidence that niflumic acid, the most potent inhibitor of these channels in vascular myocytes (Large and Wang, 1996), also induces a complex stimulation of the channels in rabbit coronary smooth muscle cells, an effect which is masked by its faster inhibitory action but can be revealed upon rapid washout of the drug. Our work highlights the caveats about the use of this tool to study the physiological role of Cl_{Ca} channels. In studies carried out to investigate their functional role, NFA was shown to alleviate agonist-induced tone, which is caused by a sustained elevation in $[Ca^{2+}]_i$. Such a condition reduces the ability of NFA to block $I_{Cl(Ca)}$ compared with its effect on STICs (Hogg et al., 1994a; Greenwood and Large, 1995). Our experimental and simulated data support the notion that the reduced efficacy of NFA as an inhibitor may be caused by partial stimulation of the channels in the presence of the drug. Therefore, lack of effect of NFA in contraction studies with multicellular preparations should not be taken as evidence against a physiological role of Cl_{Ca} in determining vascular smooth muscle tone.

Acknowledgments

We are thankful to Dr. Rémy Sauvé for helpful comments and suggestions during the course of this work.

References

Arreola J, Melvin JE, and Begenisich T (1996) Activation of calcium-dependent chloride channels in rat parotid acinar cells. *J Gen Physiol* **108:**35–47.

Britton FC, Ohya S, Horowitz B, and Greenwood IA (2002) Comparison of the properties of CLCA1 generated currents and $I_{Cl(Ca)}$ in murine portal vein smooth muscle cells. *J Physiol* **539:**107–117.

Callamaras N and Parker I (2000) Ca^{2+}-dependent activation of Cl^- currents in *Xenopus* oocytes is modulated by voltage. *Am J Physiol* **278:**C667–C675.

Criddle DN, deMoura RS, Greenwood IA, and Large WA (1996) Effect of niflumic acid on noradrenaline-induced contractions of the rat aorta. *Br J Pharmacol* **118:**1065–1071.

Criddle DN, deMoura RS, Greenwood IA, and Large WA (1997) Inhibitory action of niflumic acid on noradrenaline- and 5-hydroxytryptamine-induced pressor responses in the isolated mesenteric vascular bed of the rat. *Br J Pharmacol* **120:**813–818.

Cruickshank SF, Baxter LM, and Drummond RM (2003) The Cl^- channel blocker niflumic acid releases Ca^{2+} from an intracellular store in rat pulmonary artery smooth muscle cells. *Br J Pharmacol* **140:**1442–1450.

Dai Y and Zhang JH (2001) Role of Cl^- current in endothelin-1-induced contraction in rabbit basilar artery. *Am J Physiol* **281:**H2159–H2167.

Gordienko DV, Zholos AV, and Bolton TB (1999) Membrane ion channels as physiological targets for local Ca^{2+} signalling. *J Microsc* **196:**305–316.

Greenwood I, Ledoux J, and Leblanc N (2001) Differential regulation of Ca^{2+}-activated Cl^- currents in rabbit arterial and portal vein smooth muscle cells by Ca^{2+}-calmodulin-dependent kinase. *J Physiol* **534:**395–408.

Greenwood IA and Large WA (1995) Comparison of the effects of fenamates on Ca-activated chloride and potassium currents in rabbit portal vein smooth muscle cells. *Br J Pharmacol* **116:**2939–2948.

Hirakawa Y, Gericke M, Cohen RA, and Bolotina VM (1999) Ca^{2+}-dependent Cl^- channels in mouse and rabbit aortic smooth muscle cells: regulation by intracellular Ca^{2+} and NO. *Am J Physiol* **277:**H1732–H1744.

Hogg RC, Wang Q, and Large WA (1994a) Action of niflumic acid on evoked and spontaneous calcium-activated chloride and potassium currents in smooth muscle cells from rabbit portal vein. *Br J Pharmacol* **112:**977–984.

Hogg RC, Wang Q, and Large WA (1994b) Effects of Cl channel blockers on Ca-activated chloride and potassium currents in smooth muscle cells from rabbit portal vein. *Br J Pharmacol* **111:**1333–1341.

Jaggar JH, Porter VA, Lederer WJ, and Nelson MT (2000) Calcium sparks in smooth muscle. *Am J Physiol* **278:**C235–C256.

Kato K, Evans AM, and Kozlowski RZ (1999) Relaxation of endothelin-1-induced pulmonary arterial constriction by niflumic acid and NPPB: mechanism(s) independent of chloride channel block. *J Pharmacol Exp Ther* **288:**1242–1250.

Klöckner U (1993) Intracellular calcium ions activate a low-conductance chloride channel in smooth-muscle cells isolated from human mesenteric artery. *Pflueg Arch Eur J Physiol* **424:**231–237.

Kuruma A and Hartzell HC (2000) Bimodal control of a Ca^{2+}-activated Cl^- channel by different Ca^{2+} signals. *J Gen Physiol* **115:**59–80.

Lamb FS and Barna TJ (1998) Chloride ion currents contribute functionally to norepinephrine-induced vascular contraction. *Am J Physiol* **275:**H151–H160.

Large WA and Wang Q (1996) Characteristics and physiological role of the Ca^{2+}-activated Cl^- conductance in smooth muscle. *Am J Physiol* **271:**C435–C454.

Ledoux J, Greenwood I, Villeneuve LR, and Leblanc N (2003) Modulation of Ca^{2+}-dependent Cl^- channels by calcineurin in rabbit coronary arterial myocytes. *J Physiol* **552.3**: 701–714.

Ledoux J and Leblanc N (2002) Dual modulation of calcium-activated chloride channels by niflumic acid in rabbit coronary artery myocytes. *J Physiol* **543P:**S155.

Li L, Vapaatalo H, Vaali K, Paakkari I, and Kankaanranta H (1998) Flufenamic and tolfenamic acids and lemakalim relax guinea-pig isolated trachea by different mechanisms. *Life Sci* **62:**PL303–PL308.

Ottolia M and Toro L (1994) Potentiation of large conductance K_{Ca} channels by niflumic, flufenamic and mefenamic acids. *Biophys J* **67:**2272–2279.

Pacaud P, Loirand G, Grégoire G, Mironneau C, and Mironneau J (1992) Calcium-dependence of the calcium-activated chloride current in smooth muscle cells of rat portal vein. *Pflueg Arch Eur J Physiol* **421:**125–130.

Piper AS and Greenwood IA (2003) Anomalous effect of anthracene-9-carboxylic acid on calcium-activated chloride currents in rabbit pulmonary artery smooth muscle cells. *Br J Pharmacol* **138:**31–38.

Piper AS, Greenwood IA, and Large WA (2002) Dual effect of blocking agents on Ca^{2+}-activated Cl^- currents in rabbit pulmonary artery smooth muscle cells. *J Physiol* **539:**119–131.

Piper AS and Large WA (2003) Multiple conductance states of single Ca^{2+}-activated Cl^- channels in rabbit pulmonary artery smooth muscle cells. *J Physiol* **547:**181–196.

Remillard CV and Leblanc N (1996) Mechanism of inhibition of delayed rectifier K^+ current by 4-aminopyridine in rabbit coronary myocytes. *J Physiol* **491:** 383–400.

Remillard CV, Lupien MA, Crépeau V, and Leblanc N (2000) Role of Ca^{2+}- and swelling-activated Cl^- channels in α_1-adrenoceptor-mediated tone in pressurized rabbit mesenteric arterioles. *Cardiovasc Res* **46:**557–568.

van Renterghem C and Lazdunski M (1993) Endothelin and vasopressin activate low conductance chloride channels in aortic smooth muscle cells. *Pflugers Arch Eur J Physiol* **425:**156–163.

Yuan XJ (1997) Role of calcium-activated chloride current in regulating pulmonary vasomotor tone. *Am J Physiol* **272:**L959–L968.

Address correspondence to: Dr. Normand Leblanc, Department of Pharmacology/Mail Stop 318, Center of Biomedical Research Excellence, Savitt Medical Sciences Building, Room 50, University of Nevada School of Medicine, Reno, NV 89557-0270. E-mail: NLeblanc@med.unr.edu